34. Kuwata-Gonokami M et al. *Phys. Rev. Lett.* **95** 227401 (2005)
35. Ishihara T, Koshino K, Nakashima H *Phys. Rev. Lett.* **91** 253901 (2003)
36. Hatano T et al. *Phys. Rev. Lett.* , in press (2009); arXiv:0904.4800
37. Agranovich V M, Gartstein Yu N *Usp. Fiz. Nauk* **176** 1051 (2006) [*Phys. Usp.* **49** 1029 (2006)]
38. Simovski C R, Tretyakov S A *Phys. Rev. B* **75** 195111 (2007)
39. Smith D R et al. *Phys. Rev. B* **65** 195104 (2002)
40. Smith D R, Schurig D, Mock J J *Phys. Rev. E* **74** 036604 (2006)
41. Pendry J B *Science* **306** 1353 (2004)
42. Chen X et al. *Phys. Rev. E* **71** 046610 (2005)
43. Rill M S et al. *Nature Mater.* **7** 543 (2008)
44. Kwon D-H et al. *Opt. Express* **16** 11822 (2008)
45. Figotin A, Vitebsky I *Phys. Rev. E* **63** 066609 (2001)
46. Tikhodeev S G, Weiss T, Gippius N A, in preparation (2009)
47. Tikhodeev S G et al. *Phys. Rev. B* **66** 045102 (2002)
48. Gippius N A, Tikhodeev S G, Ishihara T *Phys. Rev. B* **72** 045138 (2005)

PACS numbers: 36.40.Gk, 73.20.Mf, **78.67.–n**
DOI: 10.3367/UFNe.0179.200909i.1007

Plasmon effects in In(Ga)N-based nanostructures

T V Shubina, S V Ivanov,
A A Toropov, P S Kop'ev

In this report, we consider the influence of effects of localized plasmons in metallic nanoparticles on optical processes in In(Ga)N-based structures. The emission and absorption of light and the generation of photoinduced charge carriers is investigated; data on the estimation of the averaged enhancement in InN/In nanocomposites are given.

Plasmonics is a rapidly developing field of applied physics and nanotechnology characterized by the use of effects related to collective oscillations of conduction electrons in metallic structures (plasmons), frequently for quite uncommon applications [1]. The many-sidedness of plasmonics is manifested in various applications such as the realization of media with a negative refractive index [2], the creation of markers used in decoding human genome [3], the enhancement of the luminescence of organic semiconductors [4], an increase in the efficiency of photodetectors [5] and light-emitting diodes [6], controlling liquid-crystal layers [7], and the generation of emission in the terahertz range [8]. Of great interest are also the fundamental properties of plasmonic metastructures, for example, the formation of strong plasmon–polariton resonances, which can be efficiently controlled by changing their structure [9, 10].

There is one additional promising avenue for the realization of the potential of plasmonics: the creation of single-photon sources that can work at room temperature. The local enhancement of an electromagnetic field by plasmons and, correspondingly, an increase in the rate of spontaneous recombination near a metallic surface are analogs of the Purcell effect [11] in microresonators. We note that a reproducible production of microresonators with quantum dots based on wide-gap semiconductors for the same purpose is at present quite problematic.

Here, we consider optical effects in semiconductor layers and nanocomposites caused by localized plasmons (Mie resonances) excited in metallic nanoparticles. The use of particles instead of a continuous film has some advantages [12]. In particular, because of the curvature of the particle surfaces, the interaction of plasmonic excitation and light emission, forbidden due to a difference in their wave vectors, is then allowed. In essence, the study whose results are presented in this report, especially in the part that concerns nanocomposites, is a continuation of the investigation of InN layers with spontaneously formed In clusters [13–19]. In the course of this investigation, we discovered Mie resonances in the spectra of thermally detected optical absorption (TDOA) and established that the plasmons exert a noticeable influence on the emission. For illustration, Fig. 1 depicts combined images obtained via scanning electron microscopy (SEM) and micro-cathodeluminescence (micro-CL) studies of one and the same region of an InN layer. These images show an enhancement of infrared micro-CL near metallic clusters and near pores surrounded by In precipitates.

Current studies are mainly conducted using two systems: (1) InGaN and an Au nanoparticle, and (2) InN with specially formed In clusters. The choice of these pairs of materials is by no means accidental. The energy of plasmonic resonances in Au particles is close to the energy of excitonic transitions in layers of the solid alloy $In_{0.25}Ga_{0.75}$. Indium as a plasmonic metal is less known than gold. But, the applicability of a metal for the amplification of optical processes is determined by the oscillator strength of plasma resonance. The spectral dependence of this parameter can be described by the ratio of the real part of the complex dielectric function of metal to its imaginary part, $|\mathrm{Re}\,\varepsilon|/\mathrm{Im}\,\varepsilon$. In the infrared range (0.7–1 eV), where radiative optical transitions are observed in InN, this ratio for In is not less than that for Au in the visible range (about 2 eV) (Fig. 2).

An increase in the efficiency of emission implies the formation of coupled localized plasmon–radiating dipole states. For the radiative plasmon decay, the metallic particle can act as a radiating antenna; but in the case of the dominance of a nonradiative decay (with large internal losses of the particle), the coupling can quench emission of the radiating dipole. The balance between these components depends, among other factors, on the particle size [20]. In the general case, to guarantee the interaction of the radiating dipole and localized plasmon, a number of conditions must be

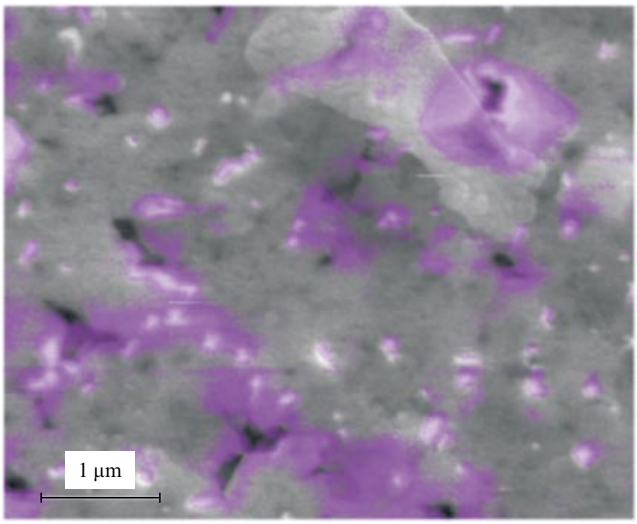

Figure 1. Superimposed images of the same region of a layer of InN obtained by SEM and micro-CL. The clusters and pores are respectively seen as bright and dark spots. The violet spots (in the electronic version of the paper at http://www.ufn.ru) correspond to intense infrared (0.75 eV) cathodoluminescence.

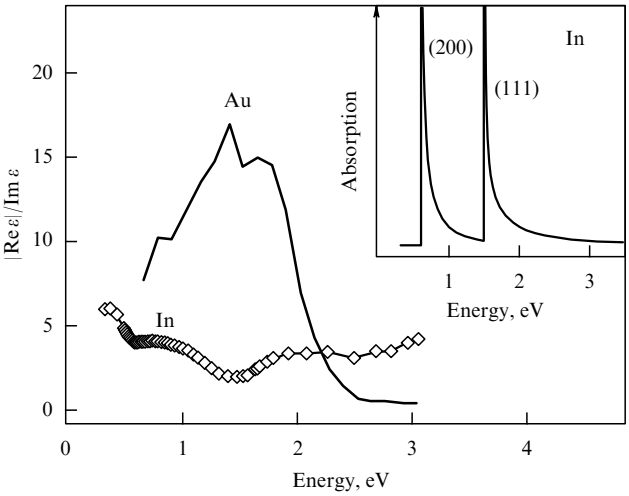

Figure 2. $|\mathrm{Re}\,\varepsilon|/\mathrm{Im}\,\varepsilon$ spectra for Au and In. The inset shows the absorption spectrum of In (without taking the electron scattering into account) due to (200) and (111) transitions between parallel bands.

satisfied, such as (1) the spatial proximity of the dipole and metallic particle, (2) the correct orientation of the dipole relative to the direction of the plasmon polarization, and (3) the coincidence of resonance frequencies.

In the approximation of a metallic cluster by an ellipsoid of revolution (spheroid) (with c being the semiaxis of revolution, and the equatorial semiaxes a and b being equal to each other), the frequency ω_i of the plasmon polarized along the ith axis of the spheroid ($i = x, y, z$) is determined by the resonance condition $\varepsilon(\omega) = -\varepsilon_1(L_i^{-1} - 1)$, where $\varepsilon_1(\omega)$ is the permeability of the environment and L_i is the depolarizing factor depending on the ratio of the lengths of the axes. The approximated expression for the frequency is written as [21]

$$\omega_i = \omega_\mathrm{p}\left[\varepsilon_\infty + \varepsilon_1(L_i^{-1} - 1)\right]^{-1/2}, \tag{1}$$

where ω_p and ε_∞ are the plasma frequency and the dielectric constant of the bulk metal. According to Eqn (1), ω_i depends substantially on the permeability of the environment and on the shape of the cluster. For example, the plasmonic frequency in bulk indium corresponds to 11.2 eV, and in a spherical In cluster located in InN ($\varepsilon_1 \sim 8$), the Mie resonance is at 2.8 eV. Resonances in clusters with the ratio c/a that considerably differs from unity fall into the infrared range if the plasmon is polarized along the longer axis of the spheroid.

In the first approximation, the plasmonic enhancement of luminescence and absorption is proportional to $|g|^2$, where $g = E/E_0$ is defined as the ratio of the local electric field to the field of the incident light wave E_0 [22]. With the polarization along the ith axis, the partial factor of field enhancement in the vicinity of the ith pole of the spheroid is given by

$$|g_i(\omega)| = \left|\frac{\varepsilon(\omega)}{\varepsilon_1(\omega) + L_i\big(\varepsilon(\omega) - \varepsilon_1(\omega)\big)}\right|. \tag{2}$$

At the resonance frequency ω_i, the partial factor $|g_i(\omega)|$ reaches the value $L_i^{-1}|\mathrm{Re}\,\varepsilon|/\mathrm{Im}\,\varepsilon \gg 1$. Generally, the enhancement factor $|g_i(\omega, \mathbf{r})|$ as a function of position $\mathbf{r}$ on the surface of the spheroid varies from the value given by Eqn (2) to the extremely small value $L_i^{-1}|\mathrm{Re}\,\varepsilon_1|/\mathrm{Im}\,\varepsilon \sim 1$ at the pole of an orthogonal axis (not equal to the ith axis) [19, 23].

The application of near-field scanning optical microscopy has allowed investigating the interaction of a localized plasmon in a single Au particle with a limited number of excitonic dipole transitions in an InGaN layer [24]. The layers were grown by the method of molecular beam epitaxy (MBE) using a regime that facilitates the formation of a nanocolumnar relief of the surface [25], which was confirmed by the data of transmission electron microscopy (TEM) (Fig. 3a). Fluctuations of the solid alloy composition led to the appearance of deeply localized states, similar to quantum dots [26]. The use of a Nanonics CryoView 2000 microscope allowed simultaneously obtaining maps of the intensity of microphotoluminescence (micro-PL) and a three-dimensional relief of the surface. A gold nanoparticle of a spheroidal shape, from 50 to 200 nm in size, was attached to the tip of a nonaperturate probe. This allowed precisely positioning the particle with respect to the InGaN layer.

The basic result of this experiment was the observation of an enhancement of the emission intensity as the gold particle approached the surface of the InGaN layer (Fig. 3b). In addition, the appearance of narrow lines in the low-temperature spectra, corresponding to the recombination of single excitons, was noted, which is a prerequisite for investigating the InGaN/Au system for the purpose of creating single-photon emitters. We note that the intensity of photoluminescence at room temperature was enhanced by a factor of several tens, whereas the previous studies of single

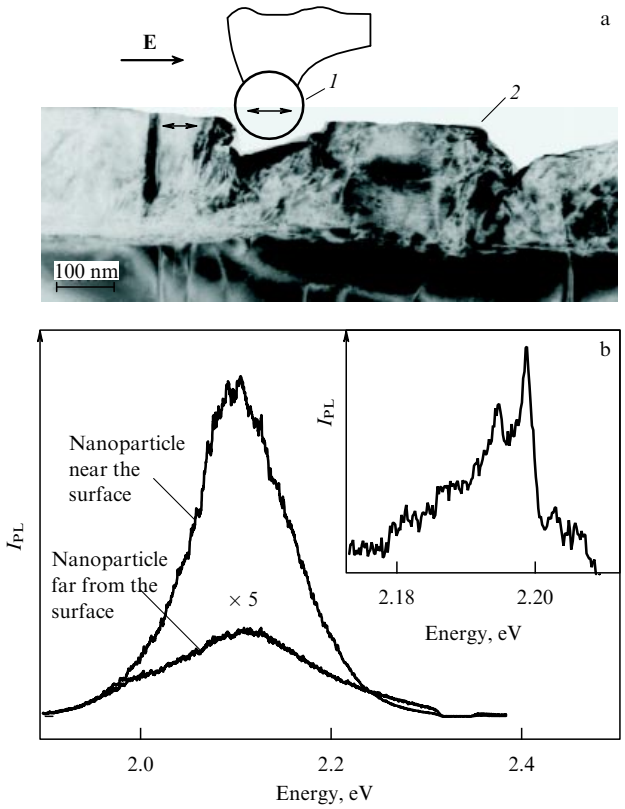

Figure 3. (a) A schematic of a probe with an Au nanoparticle (*1*), shown along with a TEM image (*2*) of the transverse section of a layer of InGaN. The left right arrows correspond to the orientation of the dipole in the layer and to the polarization of the plasmon in the particle for case of effective enhancement. (b) Micro-CL spectra measured for the cases where the Au nanoparticle is located near and far from the layer surface (at $T \approx 300$ K). The inset show narrow lines of excitonic photoluminescence in the low-temperature spectrum ($T = 12$ K).

molecules of organic dyes and colloidal quantum dots showed only a moderate (up to a few times) enhancement [27, 28]. Possibly, one of the reasons for this difference is the roughness of the samples being investigated. A comparison of the maps of photoluminescence intensity with images obtained by atomic force microscopy registered for the same region showed that the brightest spots of photoluminescence typically corresponded to dips in the relief into which the tip of the probe could sink. We note that according to electrodynamics, precisely in such a configuration the plasmon in the metallic particle polarized along the electric field vector can efficiently interact with the dipole of the exciton in the case of confocal optical microscopy. We also note that the enhancement observed for Au particles with the diameter 100 nm was absent for particles with the diameter 50 nm. This agrees well with the estimation using the model in [29]. The critical size of the spherical Au particle that allows enhancement is close to 100 nm.

Studying InN/In nanocomposites allowed understanding the specific features of the action of plasmonic resonances on the basic optical processes (emission, absorption, generation of carriers by light) in the case where the metallic clusters are located inside an optically active semiconductor matrix. The most distinct results followed from the analysis of a series of structures with periodic In inserts grown by the MBE method [23]. The inserts (6 or 20 in number) had a nominal thickness from 2 to 48 monolayers (MLs); the thickness of an ML is of the order of 0.3 nm. The inserts were separated by InN layers with the thickness 25 nm, which was grown using the ratio of the flux of N to the flux of In slightly exceeding unity for the purpose of suppressing spontaneous formation of In clusters. However, the TEM data indicate that the In clusters are formed even under these conditions.

Studies of samples by the micro-CL method were conducted using a Hitachi S4300SE microscope equipped with a detector with the sensitivity threshold 0.6 eV. The critical thickness of the metallic inserts of In in InN is ~ 1 ML. If this thickness is exceeded, the flat inserts are transformed into arrays of clusters. There then occur processes of a coarsening of the clusters and their accumulation near defects with the formation of agglomerates. These agglomerates are clearly seen in SEM images as brighter regions (Fig. 4). In the sample without inserts, no visible agglomeration of clusters exists, and the CL is weak and almost uniform. The bright spots of CL always coincide with the accumulations of clusters of In. A study in the so-called spot regime of a sample with inserts 48 MLs in thickness showed that the intensity of emission at the agglomerations of the In clusters exceeds the intensity of the signal from the regions between them by a factor of 70. On the average, this sample demonstrates emission that is five times brighter than that of the layer without inserts.

In real nanocomposites, the clusters can have an arbitrary shape and orientation relative to the electric field vector. To estimate the enhancement averaged over an ensemble of clusters, we considered a model of spheroids with a random ratio of semiaxes a/c, which had an equal (unit) volume [23]. The inhomogeneously broadened enhancement spectrum $G(\omega) = \langle |g(\omega, \mathbf{r})|^2 \rangle$, determined by the full set of plasmons, was obtained by averaging over the shape of clusters specified by the axial ratio a/c. The variation of the relation between the areas of regions with small and large surface curvatures and the depth of penetration of the field into the semiconductor were also taken cuto account. The electronic structure of

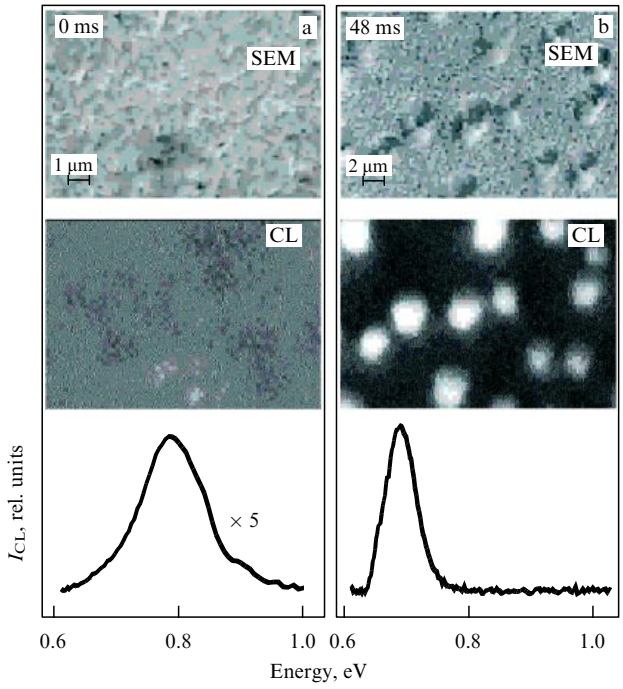

Figure 4. Comparison of an SEM image, a micro-CL pattern, and emission spectra obtained from the same region of two structures: (a) without metallic inserts; and (b) with In inserts (48 MLs thick). The bright emission spots coincide with agglomerates of In clusters.

indium is characterized by the presence of parallel regions of electron bands, between which intense transitions near the Fermi surface are possible, leading to an additional absorption in the infrared range (the (111) and (200) transitions in Fig. 2 are denoted in accordance with the classification in [30]). This feature was also taken into account in the calculations.

The maximum value of the emission and absorption enhancement coefficient $|g(\omega_i)|^2$ for an elementary plasma excitation in InN/In, according to Eqn (2), is equal to $10^3 - 10^4$ in surface regions with a large curvature. But because of the small fraction of such regions and a dispersion in the shape of the spheroids, the average enhancement in the nanocomposites does not exceed 10^2 at the energy 0.7 eV for the distribution center position $a/c = 1$ (sphere) and the distribution width $\delta < 10$. The averaged value of enhancement obtained agrees well with the data on the enhancement of micro-CL near clusters. The spectral dependences in Fig. 5 show that an increase in δ must shift the main peak in the absorption spectra into the region of lower energies and sharpen its edge, because the elementary resonances are strongest in this region. A comparison of Figs 5a and 5b illustrates the suppression of plasmonic enhancement by interband transitions in the semiconductor matrix, as was noted in [14]. The same effect comes from the transitions between parallel bands in In. This, in particular, causes the dip frequently observed in TDOA spectra [15–17] at the energy 1.5 eV, which corresponds to (111) transitions.

Metal–semiconductor nanocomposites are extremely inhomogeneous media. It can be assumed that some optical processes in them can occur in different regions, which are under different plasmon influences. The most distinct results that confirm this were obtained by a comparison of the spectra of TDOA and photocurrent in InN/In. The ther-

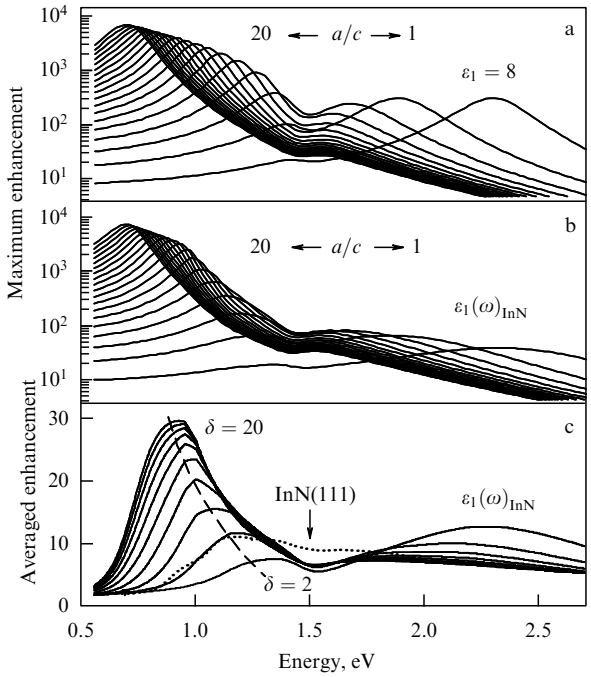

Figure 5. Spectra of maximum enhancement at various values of the axial ratio a/c (the range and the direction of the variation of a/c are shown in the figure): (a) matrix without absorption ($\varepsilon_1 = 8$); (b) matrix with absorption (energy gap $E_g \sim 1$ eV); (c) averaged spectra of enhancement calculated for various values of ($E_g \sim 1$ eV). Good agreement is observed between the calculated spectrum ($\beta = 4$) and experimental TDOA spectrum (dashed line) for the sample with a layer 48 MLs thick.

mally detected absorption technique records an increase in the sample temperature, which can be caused by two factors: interband absorption in the matrix and a dissipative decay of plasmons in metallic clusters. On the other hand, the generation of charge carriers under optical excitation arises only in the interband absorption region in InN. Therefore, the difference in the TDOA and photocurrent spectra indicates the existence of plasmonic resonances.

The photocurrent spectra were recorded under excitation by semiconductor lasers with the power 100 mW at various wavelengths. Under excitation by an incandescent lamp, the signal in the absorption edge region was negligible, in contrast to signals in other semiconductors, e.g., GaN and GaAs, in which a photocurrent can easily be excited by the lamp light in the same experimental configuration. The edges of the absorption and photocurrent spectra in these compounds were virtually coincident. But in nanocomposites, the edge of the TDOA proved to be substantially lower than the photocurrent-related edge (Fig. 6a), which can be explained by the contribution of optical losses due to a dissipative decay of plasmonic resonances. We emphasize that plasmons could enhance the rate of generation of charge carriers that form the photocurrent [31] if some density of states existed in this region. Consequently, the matrix indeed has an absorption edge shifted to the region of high energies, which can be partly caused by deviations from the stoichiometry that accompany the formation of clusters [32, 33].

At present, there is great interest in InN as a promising material for solar cells [34]. Based on the data obtained, it can be concluded that the absence of real achievements in this area is possibly connected with the neglect of spontaneous formation of In clusters. On the one hand, the plasmons in these clusters enhance photoluminescence, but on the other hand, the effective absorption edge of the matrix is shifted toward higher energies in such structures and the density of defects is increased [35]. This suppresses the photovoltaic response in InN at excitation energies less than 1.3–1.5 eV.

In InN/In nanocomposites, terahertz emission (with a frequency about 3 THz) was registered upon pumping by electric pulses [36, 37]. The measurements were conducted at the temperature 4.2 K, as was described in [38]. The nature of the terahertz emission is being refined at present. It has been reliably established that its intensity depends on the concentration n of free electrons and mobility μ (Fig. 6b). The

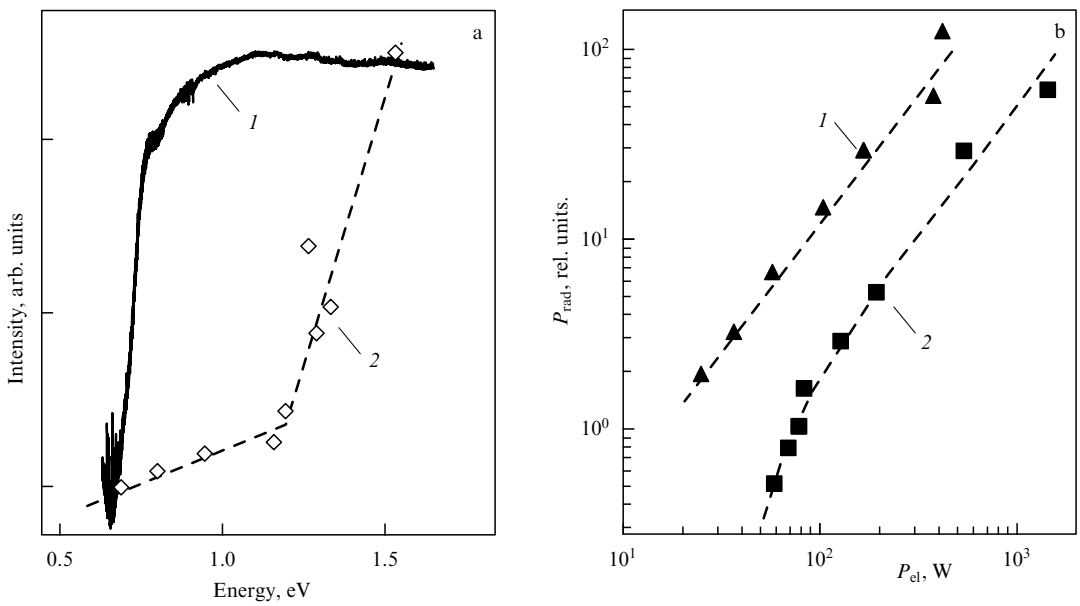

Figure 6. (a) TDOA spectra (curve *1*) and photocurrent spectra (curve *2*) in a nanocomposite InN/In. (b) The dependence of the power of terahertz emission (~ 3 THz) on the pumping power in structures with the following parameters: (*1*) $n = 5 \times 10^{18}$ cm^{-3}, $\mu = 1000$ cm^2 V^{-1} s^{-1}; and (*2*) $n = 1 \times 10^{19}$ cm^{-3}, $\mu = 200$ cm^2 V^{-1} s^{-1}.

emission spectral range agrees with the terahertz emission mechanism due to two-dimensional plasmons excited in the semiconductor matrix of the *n* type [39]. In this case, the observed increase in the intensity of terahertz emission with increasing the power of pumping can be related to an increase in the temperature of the electron gas, which facilitates thermal filling of plasmonic modes [40]. SEM studies with a subsequent Fourier transformation of images showed that the nanocomposites frequently exhibit a periodicity in the arrangement of nanocolumns, clusters, and pores. The fulfillment of the condition for the Bragg diffraction on structural inhomogeneities can favor an effective generation of terahertz emission. At the same time, the radiative decay of localized plasmons in sufficiently large In clusters has characteristic times corresponding to close frequencies that can indicate the involvement of these plasmons in the emission generation process.

We have considered effects related to the excitation of localized plasmons in metallic nanoparticles and their interaction with dipole transitions in a semiconductor. Experimental results are given for systems based on In(Ga)N. However, preliminary studies show that similar results can also be obtained for other semiconductors. This opens up great possibilities for the application of plasmonic effects in optoelectronics.

Acknowledgments. We are grateful to the researchers who took part in this work, in particular, to N A Gippius, V A Shalygin, V A Kosobukin, and T A Komisarova. This work was supported in part by the Russian Foundation for Basic Research (project Nos 07-02-00786a and 09-02-01305a) and by the Presidium of the Russian Academy of Sciences (program No. 27).

References

1. Ozbay E *Science* **311** 189 (2006)
2. Shalaev V M *Nature Photon.* **1** 41 (2007)
3. Wabuyele M B, Vo-Dinh T *Anal. Chem.* **77** 7810 (2005)
4. Bellessa J et al. *Phys. Rev. Lett.* **93** 036404 (2004)
5. Hetterich J et al. *IEEE J. Quantum Electron.* **43** 855 (2007)
6. Shen K-C et al. *Appl. Phys. Lett.* **93** 231111 (2008)
7. Kamaga C et al. *Appl. Phys. Lett.* **91** 173119 (2007)
8. Chen H-T et al. *Nature* **444** 597 (2006)
9. Christ A et al. *Phys. Rev. Lett.* **91** 183901 (2003)
10. Christ A et al. *Nano Lett.* **8** 2171 (2008)
11. Purcell E M *Phys. Rev. B* **69** 681 (1946)
12. Klimov V V *Usp. Fiz. Nauk* **178** 875 (2008) [*Phys. Usp.* **51** 839 (2008)]
13. Shubina T V et al. *Phys. Rev. Lett.* **92** 117407 (2004); **95** 209901 (2005)
14. Shubina T V et al. *Phys. Rev. Lett.* **93** 269702 (2004)
15. Shubina T V et al. *Phys. Status Solidi A* **202** 2633 (2005)
16. Shubina T V et al. *Phys. Status Solidi A* **203** 13 (2006)
17. Shubina T V et al. *J. Cryst. Growth* **288** 230 (2006)
18. Bartel T P et al. *Appl. Phys. Lett.* **91** 101908 (2007)
19. Shubina T V et al. *Phys. Status Solidi C* **4** 2445 (2007)
20. Crowell J, Ritchie R H *Phys. Rev.* **172** 436 (1968)
21. Kreibig U, Vollmer M *Optical Properties of Metal Clusters* (Berlin: Springer, 1995)
22. Moskovits M *Rev. Mod. Phys.* **57** 783 (1985)
23. Shubina T V et al. *Phys. Rev. B* **79** 153105 (2009)
24. Toropov A A et al. *Phys. Rev. Lett.* **103** 037403 (2009)
25. Jmerik V N et al. *J. Cryst. Growth* **301–302** 469 (2007)
26. Ivanov S V et al. *J. Cryst. Growth* **301–302** 465 (2007)
27. Lakowicz J R *Anal. Biochem.* **298** 1 (2001)
28. Farahani J N et al. *Phys. Rev. Lett.* **95** 017402 (2005)
29. Gersten J, Nitzan A *J. Chem. Phys.* **75** 1139 (1981)
30. Golovashkin A I et al. *Zh. Eksp. Teor. Fiz.* **51** 1623 (1966) [*Sov. Phys. JETP* **24** 1093 (1967)]
31. Westphalen M et al. *Solar Energy Mater. Solar Cells* **61** 97 (2000)
32. Shubina T V et al. *Phys. Status Solidi A* **202** 377 (2005)
33. Shubina T V et al. *Phys. Status Solidi C* **4** 2474 (2007)
34. Wu J et al. *J. Appl. Phys.* **94** 6477 (2003)
35. Komissarova T A et al. *Fiz. Tekh. Poluprov.* **43** 304 (2009) [*Semicond.* **43** 285 (2009)]
36. Shubina T V et al., in *Trudy 1-go Mezhdunar. Foruma po Nanotekhnologiyam, Moskva, 3–5 Dekabrya 2008* (Proc. 1st Int. Forum on Nanotechnologies) (Moscow: Rusnanotekh, 2008) p. 183
37. Shubina T V et al. *Izv. Ross. Akad. Nauk, Ser. Fiz.* **74** 68 (2010)
38. Shalygin V A et al. *Appl. Phys. Lett.* **90** 161128 (2007)
39. Mikhailov S A *SPIE Proc.* **3828** 139 (1999)
40. Höpfel R A, Vass E, Gornik E *Phys. Rev. Lett.* **49** 1667 (1982)

PACS numbers: 42.25.Fx, 78.20.Ls, **78.67.–n**
DOI: 10.3367/UFNe.0179.200909j.1012

Resonance scattering of light in nanostructured metallic and ferromagnetic films

V V Kurin

1. Introduction

In this report, we show that magnetooptical effects can be considerably enhanced in composite nanostructured metamaterials and ferromagnetic photonic crystals. The factors responsible for the enhancement can be both individual resonances in nanoparticles (plasma or geometrical) and collective resonances caused by multiple-scattering effects in lattices of nanoinhomogeneities.

Magnetooptical effects, which consist of a change in light polarization upon interaction with ferromagnetic materials, have been intensely studied for a sufficiently long time and are used in practice for the magnetooptical recording of information [1].

It seems obvious that magnetooptical effects can be substantially enhanced in nanostructured composite materials due to electrodynamic resonance effects, which have been given increased attention recently [2]. The nature of resonances can be different. In particular, these can be resonances connected with the excitation of natural modes of individual nanoinhomogeneities. An example of an enhancement of magnetooptical effects caused by individual resonances in a medium consisting of ferromagnetic nanospheres was first considered in Ref. [3].

Here, we demonstrate that an enhancement of magnetooptical effects can also be caused by resonance effects of another nature, such as the excitation of slowed-down waveguide modes, resonance scattering by nanowaveguides, and multiple scattering effects.

To demonstrate the effects of resonance enhancement of magnetooptical effects, we consider a simple model of an artificial medium consisting of a ferromagnetic film with cylindrical holes, assuming that the magnetization vector is directed along the normal to the film and the sizes of inhomogeneities are less than both the wavelength and the skin depth in the metal. Figure 1 shows a schematic of the scattering of an electromagnetic wave by such a structure and the basic excited waves.